PROCEEDINGS OF SPIE

SPIEDigitalLibrary.org/conference-proceedings-of-spie

Laser conditioning of UV anti-reflective optical coatings for applications in aerospace

Nils Bartels, Paul Allenspacher, Wolfgang Riede

Nils Bartels, Paul Allenspacher, Wolfgang Riede, "Laser conditioning of UV anti-reflective optical coatings for applications in aerospace," Proc. SPIE 10805, Laser-Induced Damage in Optical Materials 2018: 50th Anniversary Conference, 108051Q (16 November 2018); doi: 10.1117/12.2326782

SPIE.

Event: SPIE Laser Damage, 2018, Boulder, Colorado, United States

Downloaded From: https://www.spiedigitallibrary.org/conference-proceedings-of-spie on 11/29/2018 Terms of Use: https://www.spiedigitallibrary.org/terms-of-use

Laser conditioning of UV anti-reflective optical coatings for applications in aerospace

Nils Bartels*, Paul Allenspacher, Wolfgang Riede
German Aerospace Center (DLR), Pfaffenwaldring 38-40, 70569 Stuttgart, Germany

ABSTRACT

In this work we study the effect of laser conditioning on laser-induced damage of ion-beam sputtered, anti-reflection coated laser optics with ns-pulsed laser radiation at a wavelength of 355 nm. With respect to applications in aerospace, measurements were performed under high vacuum. At laser fluences below 20 J/cm^2, laser-induced damage appears as pin-point damage (small explosion pits with sizes in the range of 1 µm), sometimes referred to as "grey haze". We find that ramped laser conditioning is an effective tool to reduce not only the abundance but also the average size of pin-point damage at laser fluences exceeding the optic's unconditioned laser-induced damage threshold. We discuss our results in the context of the small absorber model for damage crater formation.

Keywords: Laser-induced damage, ion-beam sputtering, anti-reflection coating, aerospace, radiation, crater formation

1. INTRODUCTION

The understanding, mitigation and risk-assessment of laser-induced damage in optical coatings for high-power laser systems is a key topic for many scientific (e.g. nuclear fusion[1], particle physics[2]) and industrial (e.g. lithography[3], material processing) applications, as well as for laser development in general. A particular focus of the Laser Optics Test Center of the DLR is the advancement and qualification of optics for laser systems used in air- and spacecraft missions. For example, we have recently selected and qualified all relevant laser optics for the Atmospheric Laser Doppler LIDAR Instrument (ALADIN)[4,5], which was launched to space aboard the Aeolus wind satellite on August 22nd 2018, as part of ESA's Earth Explorer Missions.

Some of the most mission-challenging parts in space borne laser systems for the ALADIN as well as future space lasers are optical components with anti-reflection coatings for ultra-violet (UV) laser radiation. For this purpose, almost all space optics are coated via Ion Beam Sputtering (IBS), as the high kinetic energy deposition of this coating technology produces dense coatings, which have been shown to withstand the harsh environmental conditions (e.g. ultra-high vacuum[6], energetic radiation[7], atomic oxygen and hydrocarbon contaminants) encountered in space applications.

Laser-induced damage in transparent optical materials is driven by absorption from nanometer sized defects or impurities almost inevitably produced during the manufacturing process of the optical substrates and coatings.[8–10] From our experience in damage testing of optics from different suppliers, many optical coatings and even pure substrates show small damages with damage sizes in the range of 1 µm, when irradiated with laser fluences of a few J/cm^2. This type of damage morphology is sometimes referred to as "grey haze"[11], "micro-pits"[12] or "pin-point damage"[13] in the literature. The most likely origin of these damages is that they emerge from residual particles (e.g. from CeO_2, a typical polishing material[14]) or subsurface damage (SSD).[15–17] In fact, SSD and particle contamination might be closely related, because impurities can be trapped in the subsurface voids.[18]

While the ultimate goal in the manufacturing of optical coatings is to entirely avoid such residual particles, cleaning is always just a form of dilution and some particles and defects will remain in any optical coating. Thus, we underwent some effort in order to study the formation of micro-pits in Al_2O_3/SiO_2 IBS anti-reflection coatings at 355 nm in more detail. In particular, we measured the density and size distributions of micro-pits formed upon laser irradiation as a function of the laser fluence and number of applied laser pulses. Furthermore, we present results of experiments in which we tested different versions of laser conditioning in order to mitigate micro-pit formation.[19–22]

*nils.bartels@dlr.de; phone +49 711 6862-8244; www.dlr.de

Laser-Induced Damage in Optical Materials 2018: 50th Anniversary Conference, edited by Christopher Wren Carr, Gregory J. Exarhos, Vitaly E. Gruzdev, Detlev Ristau, M.J. Soileau, Proc. of SPIE Vol. 10805, 108051Q
© 2018 SPIE · CCC code: 0277-786X/18/$18 · doi: 10.1117/12.2326782

Downloaded From: https://www.spiedigitallibrary.org/conference-proceedings-of-spie on 11/29/2018
Terms of Use: https://www.spiedigitallibrary.org/terms-of-use

2. EXPERIMENTAL

Figure 1 shows a schematic of our optical test bench used for laser induced damage testing. In short, an injection-seeded, Q-switched, diode pumped Nd:YAG laser (Innolas DPSS 500) generates nanosecond, pulsed (repetition rate of 100 Hz) infrared laser radiation at 1064 nm. The third harmonic at 355 nm ($\tau_{FWHM} = 8.5$ ns) is generated in 2 LBO crystals and the energy can be controlled via an energy attenuator which consists of a motorized, λ/2-waveplate and a polarizing beam splitter. A beam splitter redirects a fraction of the laser beam to a calibrated detector for an online measurement of the pulse energy. We use computer-controlled electronic shutters in order to expose the laser optics to a defined number of laser pulses. The laser beam is focused into the high-vacuum chamber (pressure < 1×10^{-6} mbar) with an $f = 750$ mm lens and irradiates the optical component under investigation. The vacuum chamber is mounted on an electronic xy-translation stage to allow for the irradiation of different positions on the sample. The beam profile is measured in a plane equivalent to the optical component's surface with a CCD camera.

For this particular study, we investigate commercial laser windows from the same batch with an anti-reflection coating (AR@355nm/0°, Al_2O_3/SiO_2) on the front side (uncoated back side), which was generated via ion beam sputtering (IBS). During typical laser-induced damage tests, we use an online damage detection system which consists of a chopped HeNe laser beam at 632 nm that is spatially overlapped with the damaging UV laser. In the case of a damage on the optical surface, the scatter of the red laser light increases and is detected as a lock-in amplified signal of a silicon photodiode behind the vacuum chamber. Unfortunately, for very small damages (<5 µm) the online detection is not very sensitive. Therefore, we characterize the optical damage by differential interference contrast (DIC or Nomarski) microscopy (Olympus BX61 with 50×magnifying lens) ex-situ after damage testing.

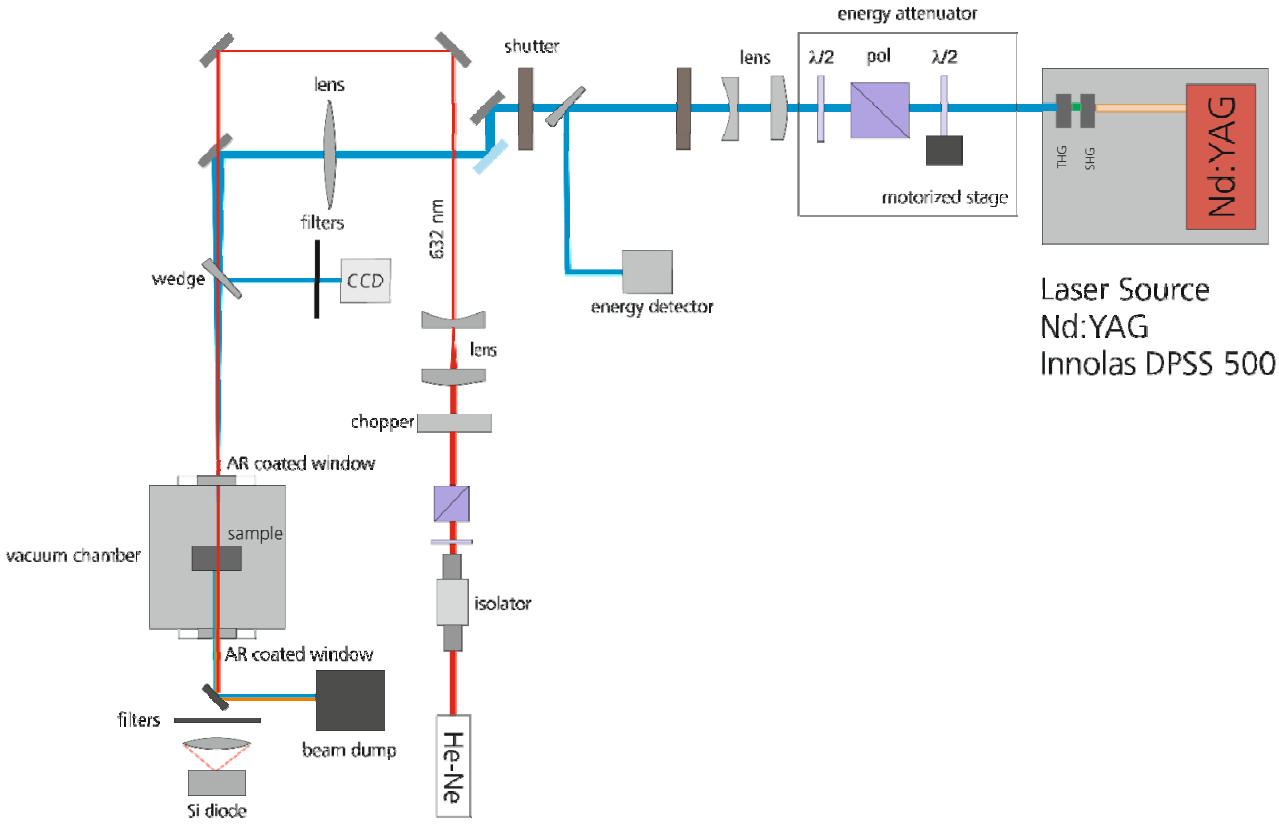

Figure 1: Experimental setup for laser-induced damage testing.

Downloaded From: https://www.spiedigitallibrary.org/conference-proceedings-of-spie on 11/29/2018
Terms of Use: https://www.spiedigitallibrary.org/terms-of-use

3. FORMATION AND SIZE DISTRIBUTIONS OF PIN-POINT DAMAGES

In a first experiment, different positions (distance between positions of 1.5 mm) on the optical sample were irradiated with predefined numbers of laser pulses (between 1 and 50.000 shots at 100 Hz) at predefined laser fluences (between 12 and 30 J/cm^2).

Figure 2 shows examples of Nomarski micrographs for different irradiation sites. The top panels (A-C) show the typical laser damage at a high laser fluence of 30 J/cm^2, which is significantly higher than the LIDT of ~7 J/cm^2 (0% damage probability at 10k pulses) for the investigated sample. After 1 laser pulse at 30 J/cm^2 (panel A) the Nomarski micrograph shows pin-point damages. After 5 laser pulses (panel B), there is an onset of delamination and after 1.000 laser pulses (panel C) we observe massive bulk damage. This is an example for a complete breakdown of the functionality of the laser optics, which would certainly lead to a mission failure of a space mission targeting laser based measurements.

As opposed to this, at a laser fluence of 15 J/cm^2 (panels D-F of Figure 2), there is also a formation of pin-point damages. However, as we will show in more detail within this work, these damages are generated within the first laser pulse and do not grow upon subsequent irradiation. In fact, it is not possible to distinguish Nomarski images taken of a spot irradiated with 1 (panel D) from a spot irradiated with 50.000 laser pulses (panel F).

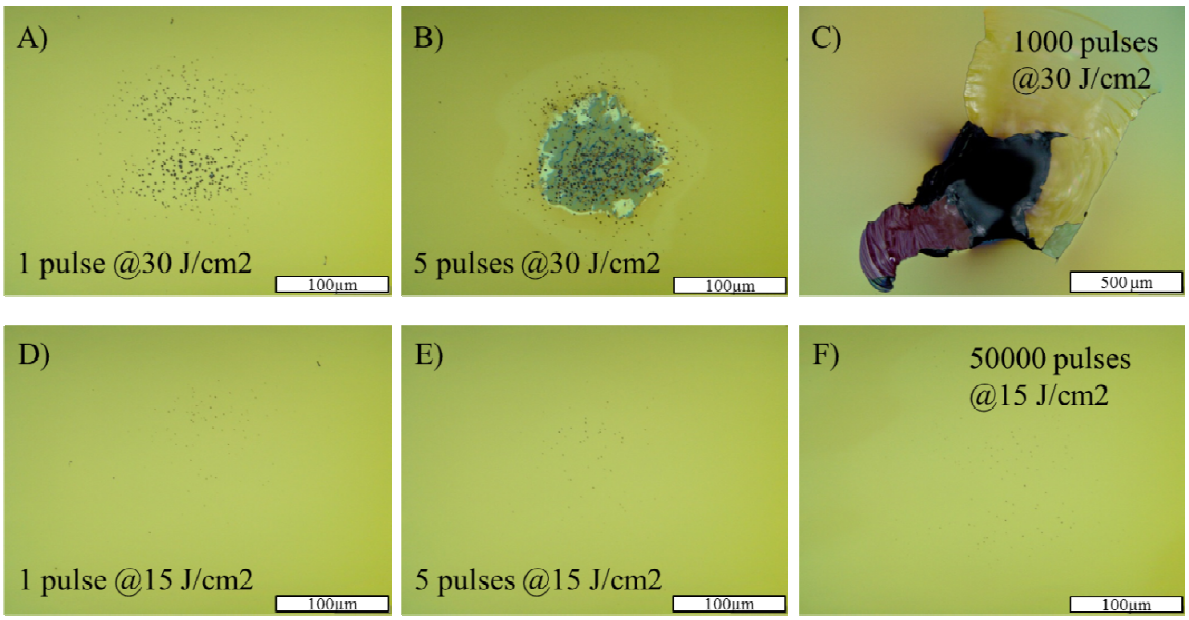

Figure 2: Nomarski micrographs showing the damage morphology after irradiation of different positions on the same IBS-coated optic for different laser fluences and pulse numbers as indicated in the figure. The scale of the micrographs is 100 µm, except for the one showing bulk damage (panel C) which has a scale of 500 µm.

Downloaded From: https://www.spiedigitallibrary.org/conference-proceedings-of-spie on 11/29/2018
Terms of Use: https://www.spiedigitallibrary.org/terms-of-use

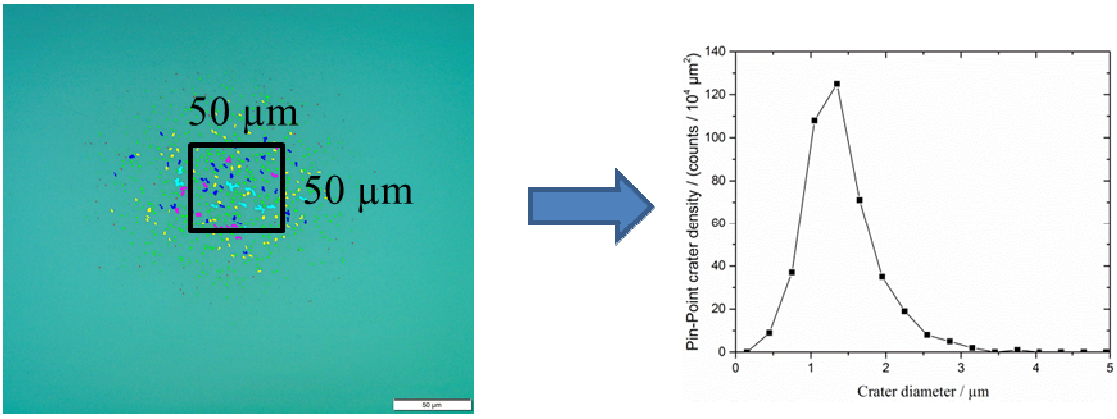

Figure 3: Concept for the extraction of size distributions from differential interference contrast (Nomarski) micrographs. Damages are detected by pattern recognition of the micrograph. Pin-point damages in the figure are colored according to their size. All detected damages within a central area of 50×50 µm2 are then binned in intervals of 0.3 µm according to their mean crater diameter to obtain a pin-point crater density distribution as shown in the panel on the right.

In order to quantify laser-induced damage, we analyze the density of micro-pits (number of micro-pits per area) within a central area of 50×50 µm^2 in which the laser fluence is above 90 % of the peak laser fluence for the laser beam diameter of $1/e^2 = 240$ µm, see Fig. 3. The analysis is performed with a native software tool of the DIC microscope, which searches for connected dark pixels representing pin-point damages. The software is set to detect damages with sizes above 0.3 µm.

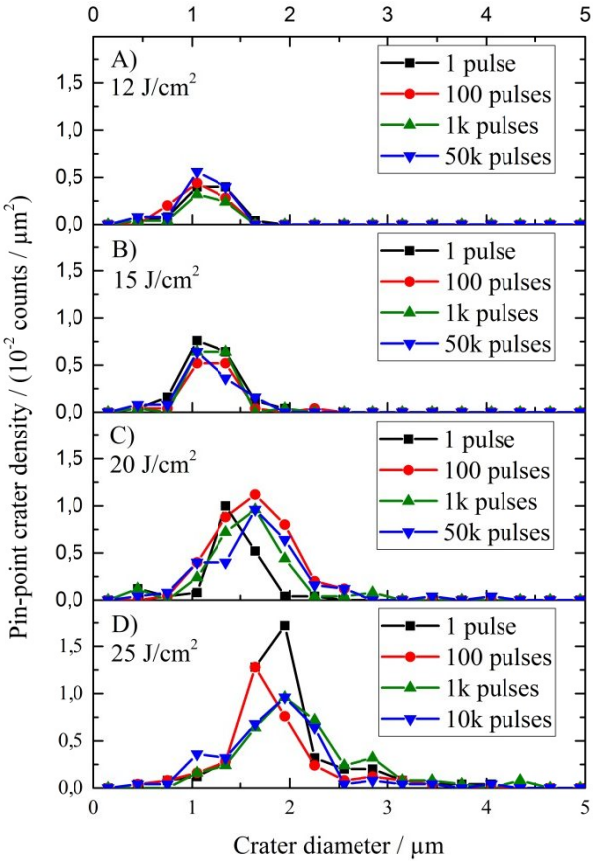

Figure 4: Crater density of pin-point damages as function of the crater diameter for different on axis peak laser fluences between 12 and 25 J/cm^2 and for different numbers of subsequently applied laser pulses as indicated in the plot legends.

Downloaded From: https://www.spiedigitallibrary.org/conference-proceedings-of-spie on 11/29/2018
Terms of Use: https://www.spiedigitallibrary.org/terms-of-use

Figure 4 shows a compilation of results for the crater density as function of the crater diameter for different on axis peak laser fluences between 12 and 25 J/cm^2 and for different numbers of subsequently applied laser pulses. Each data point represents a different position on the optical surface. In Figure 5, we furthermore extract the total number densities (top panel) and the mean diameter (middle panel) of pin-point damages, as well as the fraction of damaged surface area (bottom panel) within the analyzed 50×50 µm^2 frame.

We find that both the density and the mean diameter of pin-point damages strongly increase with increasing laser fluence. More specifically, the density rises from ~1×10^{-2}/µm^2 to ~5×10^{-2}/µm^2 and the mean diameter increases from ~1.1 µm to ~2.2 µm when comparing the data at 12 J/cm^2 with the data at 30 J/cm^2. As a result, also the fraction of damaged area increases with higher laser fluence.

In the fluence range between 12 and 20 J/cm^2, these damage parameters are essentially independent of the applied number of laser pulses. This supports the conclusion that micro-pits are predominantly formed during the first laser pulse. With subsequent laser irradiation at the same laser fluence, these damages do not grow and there are no new damages. This is because all susceptible absorbing impurities/defects in the irradiated region have already been converted into pin-point damages during the first laser pulse. At higher laser fluences such as 25 or 30 J/cm^2 we observe delamination which then leads to bulk damage (compare panels B) and D) of Figure 2) at higher pulse numbers. Therefore, the micro-pit densities, diameters and the fraction of damaged area could not be evaluated and Figure 5 does not contain data points for these cases.

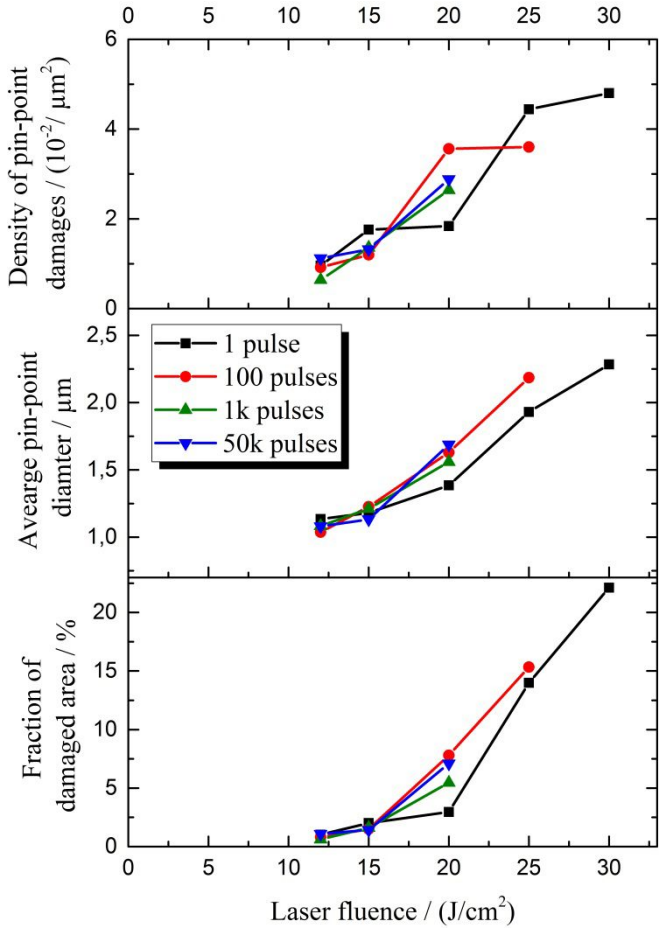

Figure 5: Density of pint-point damages (top panel), their average diameter (middle panel) and fraction of damaged area (bottom panel) in the analyzed region of 50×50 µm^2 as function of the laser fluence. The different traces in each panel correspond to different pulse numbers as given in the figure legend.

Downloaded From: https://www.spiedigitallibrary.org/conference-proceedings-of-spie on 11/29/2018
Terms of Use: https://www.spiedigitallibrary.org/terms-of-use

4. EFFECT OF LASER CONDITIONING ON SIZE DISTRIBUTIONS OF PIN-POINT DAMAGES

We decided to test two different protocols for laser conditioning and evaluated their influence on laser-induced pin-point damages.

In a first approach, each test position on the optical components' surface was irradiated with 1.000 laser pulses at a laser fluence of 6 J/cm^2 (which is below the LIDT of 7 J/cm^2) and then with 1000 laser pulses at a different laser fluence at the same position. We refer to this test protocol as "classical" (below threshold) laser conditioning. In a second approach, the laser fluence at each test position was ramped from 6 J/cm^2 to the final fluence (between 10 and 25 J/cm^2) in steps of 1 J/cm^2 with 1.000 laser pulses for each step. We refer to this test protocol as "ramped" laser conditioning.

Figure 6 compares distributions of the pin-point damage crater density for the unconditioned (top panel) laser optic with results for the "classical" (middle panel) and "ramped" (bottom panel) laser conditioned sample. Similar to the previous section of this publication, we further analyze the data by extracting the density of damages as well as their mean diameter and the fraction of damaged area, see Figure 7. We would like to mention, that compared to the data presented in Section 3, we used a larger UV laser beam diameter ($1/e^2$=340 µm) and thus also investigated a larger area (100 × 100 µm^2) for the analysis of damages.

From the data we find that while both laser conditioning protocols succeed in reducing the density and average size of pin-point damages, the results of the ramped laser conditioning protocol are much better. In particular, for a laser fluence of 15 J/cm^2, there is essentially no laser-induced damage for the ramped laser conditioning. This means that laser conditioning allows the investigated optics to be used at a laser fluence exceeding the LIDT by more than a factor of 2.

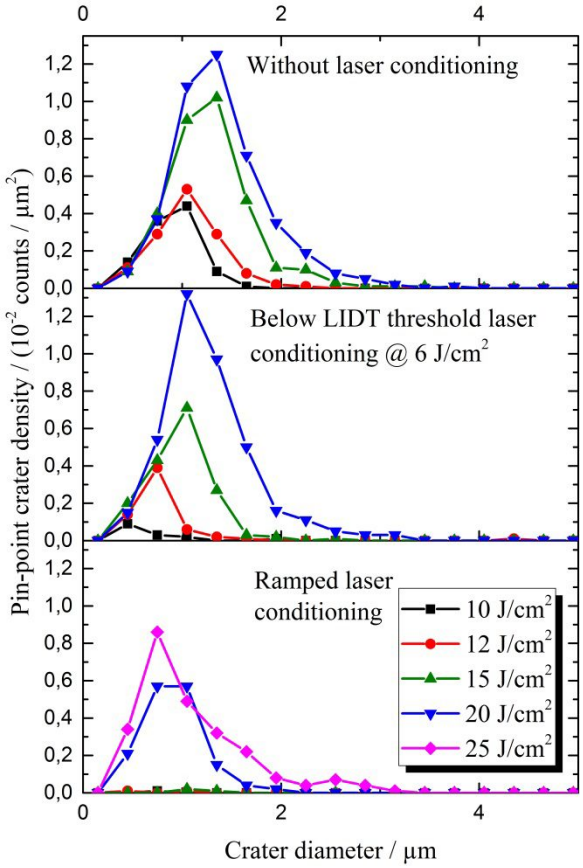

Figure 6: Comparison of size distributions for pin-point damages without (top panel) laser conditioning as well as with classical (below LIDT threshold, middle panel) and ramped (bottom panel) laser conditioning.

Downloaded From: https://www.spiedigitallibrary.org/conference-proceedings-of-spie on 11/29/2018
Terms of Use: https://www.spiedigitallibrary.org/terms-of-use

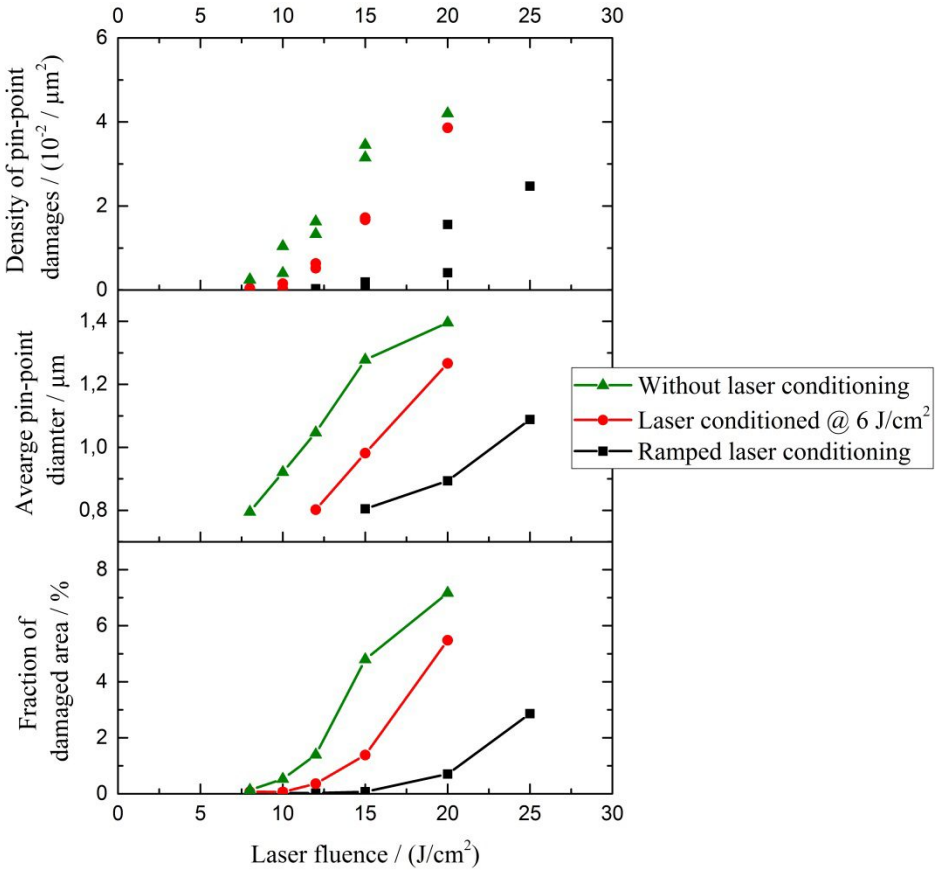

Figure 7: Density (top panel), average diameter (middle panel) and fraction of damaged area (bottom panel) in the analyzed region of 100×100 µm^2 as function of the laser fluence. We have performed two runs of the experiment and in the top panel there are thus two different data points at each fluence for the evaluated density of pin-point damages. The missing data points at 20 and 25 J/cm^2 represent delamination or bulk damage and thus could not be evaluated. For the calculation of the average diameter and fraction of damaged area we averaged the available data from the two runs.

We would like to note in passing, that we also performed a test to verify the permanence of the laser conditioning effect. For this test, we ramped the laser fluence at a position on the sample to a specific value (e.g. up to 20 J/cm^2), waited for two days (the sample was still under vacuum) and then directly exposed the sample to the specified laser fluence. We found that the second exposure did not lead to additional micro-pits. Thus, the laser conditioning effect is permanent (at least for a time of 2 days under vacuum).

5. DISCUSSION OF THE RESULTS WITHIN A SMALL ABSORBER MODEL

In this chapter we discuss our results within a model of small, localized absorbers[8–11,23–25]. Within this model, damage is initiated around nanoscale absorbers. These small absorbers (compared to larger absorbers) have a low heat capacity with respect to their absorbing surface area and thus absorption of laser radiation results in a rapidly increasing local temperature. This temperature may reach several 1.000 Kelvin, thereby generating a plasma in the vicinity of the defect.[25] This plasma itself starts absorbing energy and energy is accumulated during the laser pulse until being released in a micro-explosion. As the crack formation/micro-explosion occurs on a characteristic timescale (>10^{-8}s) longer than the laser pulse duration, the plasma around the nanoscale absorber can gather an excess energy above the threshold for crack formation.[26] This excess energy drives the micro-explosion and determines the crater size, explaining the trend that the average diameter of pin-point damages increases with higher laser fluence. In the investigated anti-reflective coating with a thickness of only ~120 nm, the damage is initiated close to the surface and material is ejected.[11]

Downloaded From: https://www.spiedigitallibrary.org/conference-proceedings-of-spie on 11/29/2018
Terms of Use: https://www.spiedigitallibrary.org/terms-of-use

The interesting question is how the increase of a laser-induced damage resistance in the studied system due to laser conditioning (observed e.g. in KTP crystals[27], bare substrates[8] and other IBS sputtered films[21]) can be explained within this small absorber model. Previously, UV laser conditioning was attributed to a mechanism in which melting of the inclusion as well as the surrounding matrix results in a dispersion of the inclusion in the host material.[8,20,26] This dispersion then leads to a decreased density of absorbed energy and thus a higher damage threshold.

An alternative explanation to this dispersion based model is that laser radiation above the laser-induced damage threshold actually leads to a small micro-explosion in any case (even in case of laser conditioning). If it is accepted that the crater size is governed by this excess energy, it is clear that in order to generate none (meaning too small to be detected) or at least only small damages, each localized absorber should be "destroyed" with the smallest possible excess energy. This explains why the ramped laser conditioning is far superior to the "classical", below laser-induced damage threshold laser conditioning. In fact, up to a laser fluence of 15 J/cm^2, the ramped laser conditioning increases the damage resistance of the material and we detect almost no change in the surface morphology.

The idea of understanding laser conditioning as a form of micro-explosion with small excess energy is not necessarily a contradiction to the dispersion based understanding of laser conditioning. The reality might be that both effects exist in the investigated optical coating and complement each other.

6. CONCLUSIONS AND OUTLOOK

We demonstrated that ramped laser conditioning is an effective tool to reduce not only the abundance, but also the average size of pin-point damages in IBS sputtered anti-reflection coated laser optics at 355 nm. The observed data is consistent with a model in which pin-point damage originates from micro-explosions at small localized absorption centers. Ramped laser conditioning is superior to below threshold laser conditioning because each defect/inclusion is destroyed with smallest possible excess energy.

An idea to further mitigate nano-absorbers in optical coatings is to apply laser conditioning already during the IBS coating process. This would allow for evaporating possible impurities and inclusions before they are even buried in the optical coating. In fact, such experiments are currently in preparation in an ESA project (ESA Contract No. 4000119563/17/NL/BJ) in cooperation with Laser Zentrum Hannover (LZH).

From our experience with laser optics for space applications, the highest risk for the long term durability of optical coatings is their resistance with respect to laser-induced molecular contamination (LIMC). In fact, we have recently shown that the localized heating of nano-inclusions can enhance LIMC via local heating, even though the nanometer-sized inclusions are not in direct contact with the contaminant.[28,29] Thus, in future work we would like to assess, whether laser conditioning (either after or during the coating process) also benefits the mitigation of laser-induced damage for high-power laser optics in "real world", space-like environments.

ACKNOWLEDGEMENTS

We greatly appreciate the support by the Aeolus laser development team (ESA).

REFERENCES

1. P. A. Baisden et al., "Large Optics for the National Ignition Facility," 1, Fusion Science and Technology **69**(1), 295–351, Taylor & Francis (2016).
2. I. A. Makhotkin et al., "Experimental study of EUV mirror radiation damage resistance under long-term free-electron laser exposures below the single-shot damage threshold," 1, Journal of Synchrotron Radiation **25**(1), 77–84 (2018).
3. M. Müller et al., "Characterisation of EUV damage thresholds and imaging performance of Mo/Si multilayer mirrors," in Proc.SPIE **8777**, pp. 8777 – 8777 – 10 (2013).
4. A. Grete Straume et al., "ESA's spaceborne lidar mission ADM-Aeolus; project status and preparations for launch," EPJ Web of Conferences **176**, 04007 (2018).

Downloaded From: https://www.spiedigitallibrary.org/conference-proceedings-of-spie on 11/29/2018
Terms of Use: https://www.spiedigitallibrary.org/terms-of-use

5. D. Wernham et al., "Verification for robustness to laser-induced damage for the Aladin instrument on the ADM-Aeolus satellite," in Proc.SPIE **10014**, pp. 10014 – 10014 – 10 (2016).
6. L. Jensen et al., "Damage threshold investigations of high-power laser optics under atmospheric and vacuum conditions," in Proc.SPIE **6403**, pp. 6403 – 6403 – 10 (2007).
7. S. F. Pellicori et al., "Development and testing of coatings for orbital space radiation environments," 4, Appl. Opt. **53**(4), A339–A350, OSA (2014).
8. J. DiJon, T. Poiroux, and C. Desrumaux, "Nano absorbing centers: a key point in the laser damage of thin films," in Proc.SPIE **2966**, pp. 2966 – 2966 – 11 (1997).
9. L. G. DeShazer, B. E. Newnam, and K. M. Leung, "Role of coating defects in laser-induced damage to dielectric thin films," 11, Applied Physics Letters **23**(11), 607–609 (1973).
10. T. Walker et al., "Impurity breakdown model in thin films," in Laser induced damage in optical materials, 1979: proceedings of a symposium **726**, p. 479, The Bureau (1980).
11. M. D. Feit et al., "Scaling relations for laser damage initiation craters," in Proc.SPIE **4347**, pp. 4347 – 4347 – 8 (2001).
12. J. M. Yoshiyama et al., "Effects of polishing, etching, cleaving, and water leaching on the UV laser damage of fused silica," in Proc.SPIE **3244**, pp. 3244 – 3244 – 10 (1998).
13. G. Batavičiūtė, M. Ščiuka, and A. Melninkaitis, "Direct comparison of defect ensembles extracted from damage probability and raster scan measurements," 10, Journal of Applied Physics **118**(10), 105306 (2015).
14. J. Neauport et al., "Polishing-induced contamination of fused silica optics and laser induced damage density at 351 nm," 25, Opt. Express **13**(25), 10163–10171, OSA (2005) [doi:10.1364/OPEX.13.010163].
15. J. Neauport et al., "Polishing-induced contamination of fused silica optics and laser induced damage density at 351 nm," 25, Opt. Express **13**(25), 10163–10171, OSA (2005).
16. D. W. Camp et al., "Subsurface damage and polishing compound affect the 355-nm laser damage threshold of fused silica surfaces," in Proc.SPIE **3244**, pp. 3244 – 3244 – 9 (1998).
17. M. Yang et al., "Reduction of the 355-nm laser-induced damage initiators by removing the subsurface cracks in fused silica," Proceedings of SPIE - The International Society for Optical Engineering **8206**, 22 (2011).
18. L. Hongjie et al., "Subsurface defects of fused silica optics and laser induced damage at 351 nm," 10, Opt. Express **21**(10), 12204–12217, OSA (2013).
19. A. Melninkaitis et al., "Laser conditioning of high reflectivity mirrors used in OPOs by 266 and 355 nm nanosecond pulses," in Proc.SPIE **7504**, pp. 7504 – 7504 – 6 (2009).
20. H. Bercegol, "What is laser conditioning: a review focused on dielectric multilayers," in Proc.SPIE **3578**, pp. 421–426 (1999).
21. D. C. Ness, T. Bittancourt, and A. D. Streater, "A year of automated LDT testing on ion beam sputtered thin film optics and laser conditioning of IBS films," in Proc.SPIE **6403**, pp. 6403 – 6403 – 13 (2007).
22. J. A. Menapace et al., "Combined advanced finishing and UV-laser conditioning for producing UV-damage-resistant fused-silica optics," in Proc.SPIE **4679**, pp. 4679 – 4679 – 13 (2002).
23. L. Gallais et al., "Investigation of nanodefect properties in optical coatings by coupling measured and simulated laser damage statistics," 5, Journal of Applied Physics **104**(5), 053120 (2008).
24. L. Jensen et al., "Spot-size dependence of the LIDT from the NIR to the UV," in Proc.SPIE **7504**, pp. 7504 – 7504 – 8 (2009).
25. C. W. Carr et al., "Localized Dynamics during Laser-Induced Damage in Optical Materials," 8, Phys. Rev. Lett. **92**(8), 087401, American Physical Society (2004).
26. S. Papernov, "Laser-induced damage in optical materials," D. Ristau, Ed., p. 44, CRC Press (2014).
27. J. Adams et al., "Wavelength and pulselength dependence of laser conditioning and bulk damage in doubler-cut KH 2 PO 4," in Laser-Induced Damage in Optical Materials: 2005 **5991**, p. 59911R, International Society for Optics and Photonics (2006).
28. F. E. Hovis et al., "Mechanisms of contamination-induced optical damage in lasers," in Proc.SPIE **2428**, pp. 2428 – 2428 – 12 (1995).
29. I. Balasa et al., "Enhancement of contamination growth and damage by absorption centers under UV irradiation," in Proc.SPIE **9237**, pp. 9237 – 9237 – 10 (2014).

Downloaded From: https://www.spiedigitallibrary.org/conference-proceedings-of-spie on 11/29/2018
Terms of Use: https://www.spiedigitallibrary.org/terms-of-use